

Systematic control of high-speed damping in doped/undoped $\text{Ni}_{81}\text{Fe}_{19}$ (50 nm) bilayer thin films

Hajung Song, Lili Cheng, and William E. Bailey^{a)}

Materials Science and Engineering Program, Department of Applied Physics, Columbia University, New York, New York 10027

(Presented on 6 January 2004)

We show that the relaxation of GHz precessional motion in soft ferromagnetic thin films can be controlled through the inhomogeneous placement of dopants. Bilayers of doped and undoped permalloy ($\text{Ni}_{81}\text{Fe}_{19}$), $\text{Ni}_{81}\text{Fe}_{19}/\text{Ni}_{81}\text{Fe}_{19}:\text{Tb}$ (Tb 5%), varied in net relaxation rate λ according to the thickness fraction of the doped layer. The behavior is roughly independent of total bilayer thickness and deposition order in the range studied (50–100 nm). The technique provides a means to control the high-speed response of magnetoelectronic devices with limited effect on signal, as magnetically active dopants can be separated from the interfaces relevant for spin transport.

© 2004 American Institute of Physics. [DOI: 10.1063/1.1669338]

I. INTRODUCTION

The ongoing demand for higher data rate (>1 GHz) in magnetoelectronic devices requires shorter times for both magnetic switching and the stabilization of the switched state. In 180° reversals of magnetization, the characteristic time for transient motion to decay out of the system is given by $2/\lambda$, where λ is the relaxation rate in GHz. Therefore moderate enhancement of λ shortens the allowed time between pulsed reversal of magnetization. Although control and understanding of damping in magnetic materials is essential for current and future magnetoelectronic devices, little work has been done in relation to manipulating materials. It was recently reported that the doping of small amount of rare-earth (RE) elements into $\text{Ni}_{81}\text{Fe}_{19}$ (50 nm) has a great effect on its damping/relaxation rate.^{1,2} It was demonstrated first¹ that using RE dopants, dynamic behavior of $\text{Ni}_{81}\text{Fe}_{19}$ could be widely controlled.

This article provides an additional configuration for the placement of dopants. We show that the damping of magnetic thin films can be controlled using a coupled bilayer structure where the dopants are confined to one layer. Tb-doped $\text{Ni}_{81}\text{Fe}_{19}$ with higher damping parameter was deposited before or after the deposition of $\text{Ni}_{81}\text{Fe}_{19}$ with lower damping parameter. By controlling relative thickness between two layers, the damping parameter of the bilayer is systematically changed. We propose that this configuration could be useful in magnetoelectronic structures, e.g., giant magnetoresistive or tunneling magnetoresistive heads or magnetic random access memory, so that dopants can be separated from ferromagnet/nonmagnet interfaces, preserv-

ing spin transport properties, but acting on magnetization dynamics through the exchange interaction.

II. EXPERIMENTS

Bilayer thin films of Tb:5% ($\text{Ni}_{81}\text{Fe}_{19}$)/ $\text{Ni}_{81}\text{Fe}_{19}$ were prepared on thermally oxidized Si substrates using a four-target, load-locked dual ion beam sputtering system. Tb:5% ($\text{Ni}_{81}\text{Fe}_{19}$) (TbNiFe) thin films were deposited by cosputtering of Tb foil (2 in. \times 2 in.) and $\text{Ni}_{81}\text{Fe}_{19}$ (NiFe) target (8 in. diameter). The Tb foil was positioned over the NiFe target using a manipulator, adjustable from outside the chamber. Relative thickness ratio of TbNiFe layer, (TbNiFe thickness)/(bilayer thickness), was changed while total bilayer thickness was fixed at 50 nm. By changing the deposition order of TbNiFe and NiFe, we tested possible effects of any lattice mismatch or different growth mode between two layers. All films were capped with 2–5 nm Ta layer to prevent oxidation. The overall film structure is, therefore, [TbNiFe x nm/NiFe 50- x nm/Ta].

Base pressure before deposition was between 6×10^{-8} and 2×10^{-7} Torr. Ar gas flow rate into the ion gun was 13 sccm and working pressure was 2×10^{-4} Torr. The ion beam current and voltage was 65 mA and 800 V, respectively. Deposition rate was about 0.4 Å/s. During the film growth, the substrate holder was rotated to enhance the film homogeneity. Magnetic field of about 20 Oe was applied to induce unidirectional anisotropy in the film plane.

Static and dynamic magnetic properties were characterized using a magneto-optic Kerr effect (MOKE) magnetometer³ and a pulsed inductive microwave magnetometer (PIMM),^{4,5} respectively. In PIMM measurement, the magnetic film, coated with photoresist, is placed on a microwave coplanar waveguide which is connected in transmission between a step pulse generator and a sampling oscillo-

^{a)} Author to whom correspondence should be addressed; electronic mail: web54@columbia.edu

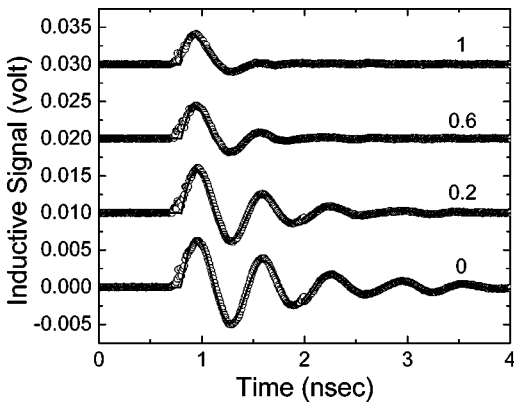


FIG. 1. Inductive signals of selected bilayer samples, [SiO₂/TbNiFe *x* nm/NiFe 50-*x* nm/Ta]. The Tb-doped thickness fraction (*x*/50) is shown on each graph (0, 0.2, 0.6, and 1). Plots are offset for comparison. Open circles are experimental data and lines are fitted data using exponentially decaying sinusoidal function. As the doped thickness fraction increases, the ring-down time and the intensity of inductive signals decrease.

scope. When a step current pulse is generated and passes by the film, it produces a fringing field which rotates the film magnetization orthogonal to the waveguide. The inductive signal V_{ind} is proportional to $(\partial M/\partial t)$, where M is the magnetization in the direction orthogonal to the waveguide. Bias field of 20 Oe was applied parallel to the easy axis, transverse to a pulse. Measured inductive signals were fitted using exponentially decaying sinusoidal functions. Spin relaxation rate λ , directly related to the damping, was approximated by this method. Similar results were given by numerical fitting using the Landau–Lifshitz equation. Details on the dynamic measurement and analysis used in this study can be found elsewhere.^{4,5}

III. RESULTS AND DISCUSSION

Figure 1 shows selected results of dynamic measurements for [TbNiFe *x*/NiFe 50-*x*/Ta] bilayers. Thickness ratio of TbNiFe to the total bilayer, *x*/50, is shown on each graph. As TbNiFe thickness increases, the oscillation and the

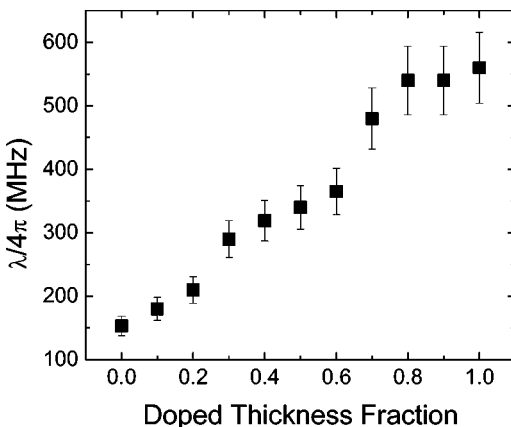


FIG. 2. Damping parameters (relaxation rates $\lambda/4\pi$) obtained from Fig. 1 are shown as a function of doped thickness fraction. The relaxation rate spans values for doped and undoped single films, and is roughly proportional to doped thickness fraction.

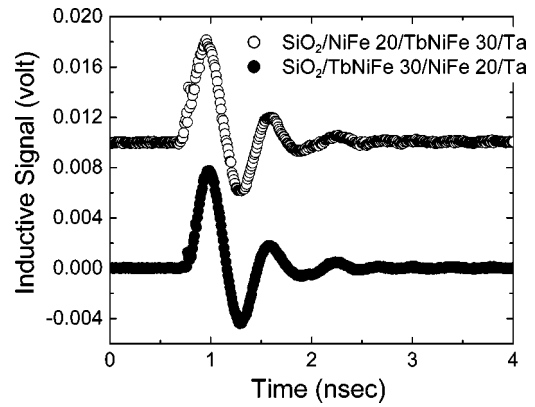


FIG. 3. Comparison of inductive signals for two equivalent bilayers with reversed deposition order as shown on the figure. Thickness unit is nanometer.

intensity of inductive signal decrease, which indicates the enhancement of damping. The behavior is more clearly shown in Fig. 2. Damping parameters used for fitting, spin relaxation rates ($\lambda/4\pi$), are shown in Fig. 2 as a function of TbNiFe thickness ratio (doped thickness fraction). It should be noted that wide variation of damping parameters, actually

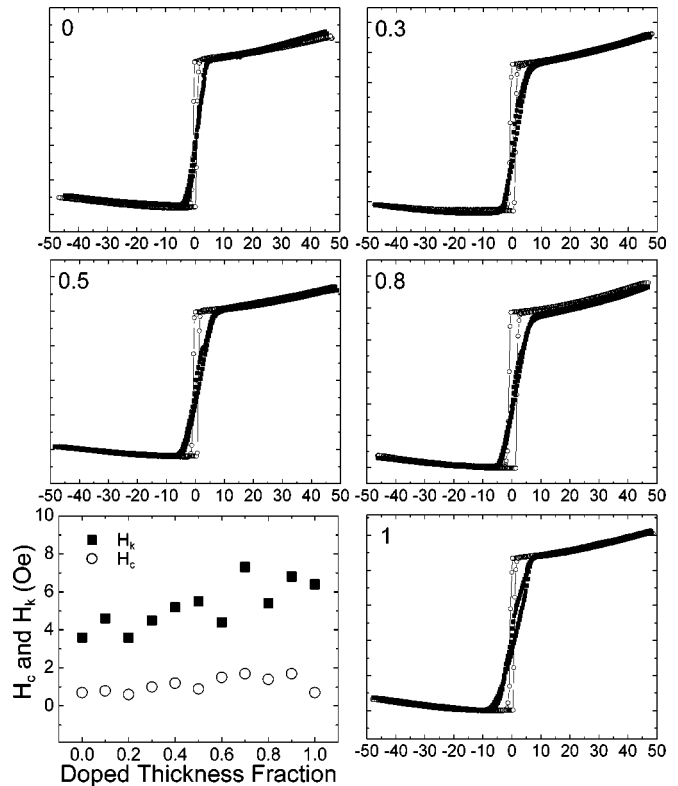


FIG. 4. Hysteresis loops, measured by MOKE, of bilayers with fixed thickness of 50 nm: [SiO₂/TbNiFe *x* nm/NiFe 50-*x* nm/Ta], the same structure as in Figs. 1 and 2. Doped thickness fractions are indicated on each graph. The Y axis is the MOKE signal in arbitrary units and the x axis is applied magnetic field in Oe. Open circles and filled squares represent easy axis loops and hard axis loops, respectively. H_c measured from easy axis loop and H_k from hard axis loop is summarized separately. In contrast to the dynamic properties shown in Fig. 2, static properties do not depend entirely on bilayer structures. Average values of H_c and H_k are 1.1 and 5.2 Oe, respectively.

in the full range between two end values of NiFe and TbNiFe, can be obtained simply by changing the thickness ratio in the bilayer structure. Furthermore, the deposition order of each layer is not important for the damping of bilayers. Two samples with the reverse deposition order show the same inductive signals in Fig. 3. This result is suggestive that growth mode or microstructure is not very important in determining the damping for these films.

Static magnetic properties were measured by MOKE and are shown in Fig. 4. Easy axis coercivities (H_c) and hard axis anisotropy fields (H_k) are summarized separately. As shown in the figure, H_c and H_k do not strongly depend on the bilayer structure. Their average values are 1.1 and 5.2 Oe, respectively. The fact that static magnetic properties are roughly conserved will foster application prospects for the future, as high-speed damping can be adjusted independently.

From our results of TbNiFe/NiFe bilayers, only the damping is significantly changed, while other properties remain roughly the same. In our bilayers, the damping parameter of TbNiFe is much higher than that of NiFe. This implies that the magnetic moment of the TbNiFe layer is more sluggish, while the magnetic moment of the NiFe layer is more mobile under the dynamic external field. In the limit of infinitely strong exchange coupling between the layers, we would expect a proportional relationship between damping λ and doped thickness fraction analogous to the proportionality between λ and RE concentration,² as no canting angle could develop and the bilayer would act as a single film. The bilayer damping, however, does not change linearly with thickness fraction, and is even discontinuous in Fig. 2. This sug-

gests more complicated or incomplete coupling, and further investigations are in progress to understand it.

IV. CONCLUSIONS

It is shown that the magnetic damping of thin films can be controlled systematically using bilayer structure with two different damping parameters. By changing the bilayer thickness ratio, damping parameters are widely tuned between two end values of each layer. The behavior is roughly independent of total bilayer thickness and deposition order in the range studied (50–100 nm). We hope our results for the control of damping using bilayer structure will give greater flexibility to design magnetoelectronic devices.

ACKNOWLEDGMENTS

This work was supported by NIST Nanomagnetodynamics (Grant No. 60NANB2D0145) and Army Research Office Young Investigator Program (ARO-43986-MS-YIP). H.S. acknowledges support from the Post-doctoral Fellowship Program of Korea Science & Engineering Foundation (KOSEF). The authors have benefitted from facilities provided by the NSF-funded MRSEC at Columbia University under Award No. DMR-0213574.

¹W. Bailey, P. Kabos, F. Mancoff, and S. Russek, *IEEE Trans. Magn.* **37**, 1749 (2001).

²S. G. Reidy, L. Cheng, and W. E. Bailey, *Appl. Phys. Lett.* **82**, 1254 (2003).

³Z. Q. Qiu and S. D. Bader, *Rev. Sci. Instrum.* **71**, 1243 (2000).

⁴T. J. Silva, C. S. Lee, T. M. Crawford, and C. T. Rogers, *J. Appl. Phys.* **85**, 7849 (1999).

⁵A. B. Kos, T. J. Silva, and P. Kabos, *Rev. Sci. Instrum.* **73**, 3563 (2002).